The RNA-binding protein Staufen1 is increased in DM1 skeletal muscle and promotes alternative pre-mRNA splicing

Aymeric Ravel-Chapuis,[1] Guy Bélanger,[1] Ramesh S. Yadava,[2] Mani S. Mahadevan,[2] Luc DesGroseillers,[3] Jocelyn Côté,[1] and Bernard J. Jasmin[1]

[1]Department of Cellular and Molecular Medicine, Faculty of Medicine, University of Ottawa, Ottawa, Ontario, K1H 8M5, Canada
[2]Department of Pathology, University of Virginia, Charlottesville, VA 22908
[3]Department of Biochemistry, University of Montreal, Montreal, Quebec H3C 3J7, Canada

In myotonic dystrophy type 1 (DM1), dystrophia myotonica protein kinase messenger ribonucleic acids (RNAs; mRNAs) with expanded CUG repeats (CUG^{exp}) aggregate in the nucleus and become toxic to cells by sequestering and/or misregulating RNA-binding proteins, resulting in aberrant alternative splicing. In this paper, we find that the RNA-binding protein Staufen1 is markedly and specifically increased in skeletal muscle from DM1 mouse models and patients. We show that Staufen1 interacts with mutant CUG^{exp} mRNAs and promotes their nuclear export and translation. This effect is critically dependent on the third double-stranded RNA–binding domain of Staufen1 and shuttling of Staufen1 into the nucleus via its nuclear localization signal. Moreover, we uncover a new role of Staufen1 in splicing regulation. Overexpression of Staufen1 rescues alternative splicing of two key pre-mRNAs known to be aberrantly spliced in DM1, suggesting its increased expression represents an adaptive response to the pathology. Altogether, our results unravel a novel function for Staufen1 in splicing regulation and indicate that it may positively modulate the complex DM1 phenotype, thereby revealing its potential as a therapeutic target.

Introduction

Myotonic dystrophy type 1 (DM1) is caused by an expansion of CUG repeats located in the 3′ untranslated region (3′UTR) of dystrophia myotonica protein kinase (DMPK) mRNAs. Pathological severity of DM1 correlates with the number of CUG repeats (Wheeler and Thornton, 2007). This expansion causes a gain of function of the mutant CUG^{exp} mRNA, which aggregates in the nucleus as ribonuclear foci, sequestering and misregulating transcription factors and RNA-binding proteins normally destined to regulate other genes and/or mRNAs (Lee and Cooper, 2009). Thus, the imbalance in cellular regulators induces a toxic cellular effect on the expression, metabolism, and/or splicing of target mRNAs, leading to the complex phenotype seen in DM1 (O'Rourke and Swanson, 2009). In particular, missplicing events can account for symptoms, such as insulin resistance and myotonia, which are linked to aberrant splicing of insulin receptor (IR) and chloride channel (ClC-1) pre-mRNAs, respectively (Ranum and Cooper, 2006).

Studies performed with transgenic mouse models support this pathogenicity model. Indeed, mice harboring the human skeletal actin (HSA) transgene containing a pathogenic number of CTG repeats (250) in the 3′UTR, called HSA–long repeat (LR), recapitulate the characteristic features associated with DM1, including nuclear retention of CUG^{exp} mRNAs and aberrant splicing of pre-mRNAs (Mankodi et al., 2000, 2002). Additional transgenic mouse models have more recently confirmed these initial observations (Seznec et al., 2001; Mahadevan et al., 2006; Orengo et al., 2008). In particular, the *GFP* transgene fused to the *DMPK* 3′UTR under the control of a tetracycline-inducible

Correspondence to Bernard J. Jasmin: jasmin@uottawa.ca

Abbreviations used in this paper: 3′UTR, 3′ untranslated region; DM1, myotonic dystrophy type 1; DMD, Duchenne muscular dystrophy; DMPK, dystrophia myotonica protein kinase; dsRBD, double-stranded RNA-binding domain; GAPDH, glyceraldehyde 3-phosphate dehydrogenase; HSA, human skeletal actin; IR, insulin receptor; LR, long repeat; qRT-PCR, quantitative RT-PCR; RIPA, radioimmunoprecipitation assay; SR, short repeat; TA, tibialis anterior; TBD, Tubulin-binding domain; WT, wild type.

The Rockefeller University Press $30.00
J. Cell Biol. Vol. 196 No. 6 699–712
www.jcb.org/cgi/doi/10.1083/jcb.201108113

promoter demonstrated inducibility and reversibility of the DM1 pathology (Mahadevan et al., 2006).

Given this toxic RNA gain-of-function model, it becomes important to identify proteins that interact with mutant transcripts and that are misregulated in the DM1 pathology. In search of specific proteins that can bind CUG repeats, a few proteins have been characterized, including CUGBP1 (Timchenko et al., 1996) and MBNL1 (Miller et al., 2000), which are both splicing regulators. In DM1, MBNL1 is sequestered in nuclei by CUG^{exp} mRNAs, thereby reducing functional MBNL1 availability in cells (Miller et al., 2000), whereas CUGBP1 expression is increased in the cytoplasm (Savkur et al., 2001). In agreement with these observations, mice deficient in MBNL1 (Kanadia et al., 2003) or overexpressing CUGBP1 (Timchenko et al., 2004; Ho et al., 2005) display symptoms and splicing abnormalities similar to those observed in DM1 patients, thus highlighting the complementary functions of misregulated CUGBP1 and MBNL1 in the DM1 pathology. In addition to regulation of alternative splicing, these RNA-binding proteins have other regulatory functions that could also negatively impact DM1, including modulation of translation and RNA stability for CUGBP1 (Timchenko et al., 2001, 2004) and micro-RNA biogenesis for MBNL1 (Rau et al., 2011). Despite the prominent roles that these two proteins play in DM1, it is reasonable to argue that additional RNA-binding proteins also interact with DMPK transcripts and are abnormally regulated in DM1 skeletal muscle.

In a previous study, we characterized the skeletal muscle expression of the RNA-binding protein Staufen1 (Bélanger et al., 2003). Although initially associated with mRNA transport (Kiebler et al., 1999), Staufen1 is now widely recognized as a multifunctional protein involved in key aspects of RNA metabolism. Indeed, we now know that Staufen1 also regulates the translational efficiency of a population of mRNAs (Dugré-Brisson et al., 2005) and the stability of transcripts via a mechanism referred to as Staufen-mediated RNA decay (Kim et al., 2005b, 2007).

Given its expression in skeletal muscle (Bélanger et al., 2003), its implication in RNA-processing events, and its ability to bind extensive RNA secondary structures, here, we hypothesize that Staufen1 may therefore be misregulated by the CUG expansion and that it may participate in the DM1 pathology. In this study, we show that Staufen1 levels are specifically increased in DM1 skeletal muscle and establish novel roles for Staufen1 in pre-mRNA splicing and in the cytoplasmic export and translation of pathological CUG^{exp} mRNAs.

Results

Staufen1 is specifically increased in skeletal muscles from DM1 mouse models and biopsies from DM1 patients

The level of several RNA-binding proteins is affected in DM1, and this is believed to be a central disease-causing mechanism. To determine whether Staufen1 is affected by the CUG^{exp} mRNA in DM1, we measured the relative levels of Staufen1 by Western blotting in skeletal muscle samples from several DM1 mouse models. The DM1 mouse models used were (a) the HSA-LR and the HSA–short repeat (SR) mice carrying 250 or 5 CUG repeats, respectively, in the 3′UTR of the *HSA* gene (Mankodi et al., 2000), (b) the DM5-313 expressing an inducible transgene with the 3′UTR of DMPK with normal CUG repeats (five repeats), while showing a DM1 phenotype (Mahadevan et al., 2006), and (c) a new DM200-68/63 expressing an inducible transgene with the 3′UTR of DMPK carrying 200 CUG repeats and displaying DM1 phenotype (unpublished data).

First, we observed an increase in the abundance of the 55-kD Staufen1 isoform in HSA-LR mice carrying 250 CUG repeats compared with control HSA-SR mice carrying only five CUG repeats and wild-type (WT) mice (Fig. 1 A). Using a different Staufen1 antibody, we similarly observed a low to background level of expression of Staufen1 in samples from the control, uninduced DM5-313 line. Induction of transgene expression in DM5-313 mice led to an increase in Staufen1 expression. The increase of Staufen1 is even more pronounced in muscles from DM200-68/63–induced mice as well as in HSA-LR mice (Fig. 1 B). Interestingly, using the same animal models, others have observed no difference in the global level of MBNL1 protein while showing an increase in CUGBP1 steady-state level in DM5-313 mice but not in HSA-LR mice (Lin et al., 2006; Mahadevan et al., 2006).

To assess the potential clinical relevance of these findings, we additionally performed Western blotting on human muscle biopsies from control and DM1 patients (Fig. 1 C). Muscle biopsies from two asymptomatic individuals contained levels of Staufen1 that are below the detection capacity of the antibody under these conditions. By comparison, two muscle biopsy samples from different individuals with adult-onset DM1 showed increased expression of Staufen1. In these experiments, the 63-kD isoform of Staufen1 was sporadically detected using both mouse and human samples with no overall trend (unpublished data). Together, these findings establish that the level of the RNA-binding protein Staufen1 is elevated in DM1 skeletal muscle.

Our initial analysis showed a systematic increase of Staufen1 expression in DM1 skeletal muscles. However, we noted variations in the extent of induction of Staufen1 in the different DM1 samples that were examined. We thus wondered whether this could be related to disease severity. To examine this possibility, we determined Staufen1 levels in additional biopsy samples from DM1 patients. As shown in Fig. 1 D, we clearly observed a trend toward greater increases in Staufen1 according to disease severity as evaluated by central nuclei, inflammation, percentage of atrophic fibers, fiber size variability, and fibrosis. To further examine this, we also analyzed several additional muscle samples from DM1 mouse models. Our quantitative analysis revealed that, indeed, Staufen1 levels were the highest in samples exhibiting the greatest pathology (Fig. 1 E). This quantitative analysis was further extended to DM1 patient samples, which clearly demonstrated the same pattern of Staufen1 expression according to disease severity (Fig. 1 F). Importantly, the increase in Staufen1 in DM1 muscle appears specific because we failed to observe such induction in biopsy samples from Duchenne muscular dystrophy (DMD) and X-linked myopathy patients (Fig. 1 D). Together, these findings establish that the level of the RNA-binding protein Staufen1 is specifically elevated in DM1 skeletal muscle.

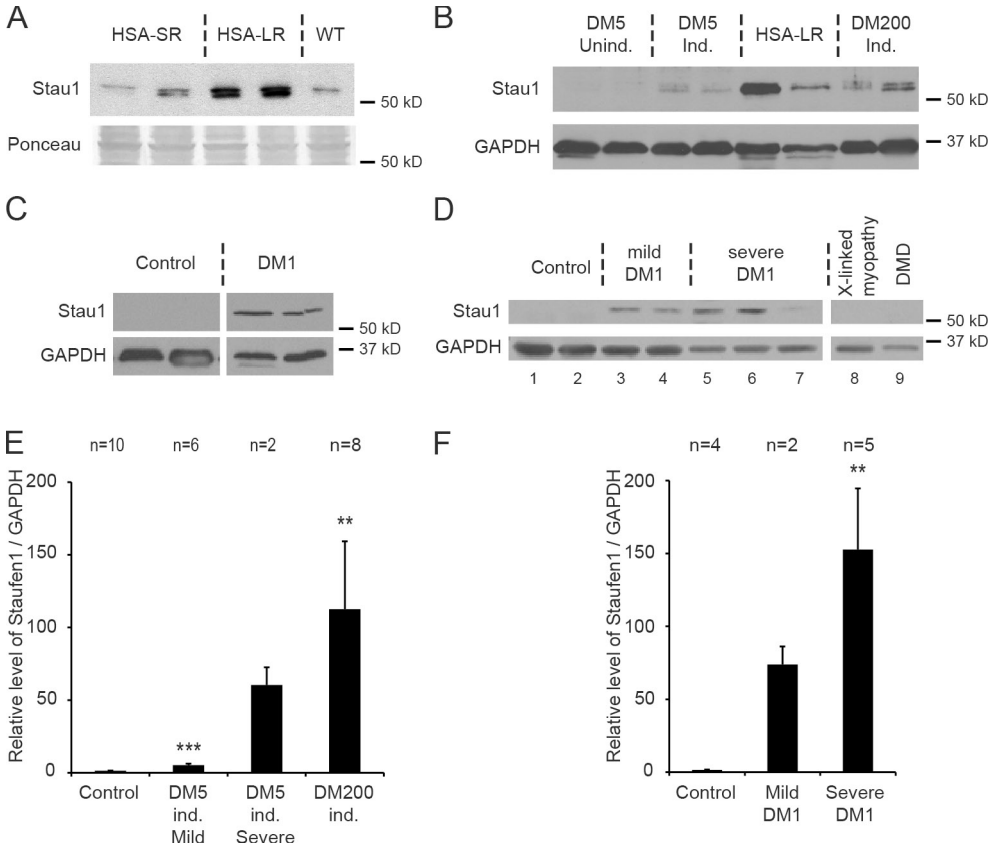

Figure 1. **Staufen1 expression is specifically increased in DM1.** (A) Western blot of muscle protein extracts showing increased Staufen1 (Stau1) in tissues from HSA-LR mice compared with HSA-SR and WT controls. Anti-Staufen1 antibody (Bélanger et al., 2003) was used. Ponceau staining was used to show equal loading. (B) Western blot of muscle protein extracts, using a different Staufen1 antibody (Abcam), showing increased Staufen1 in DM5 induced (ind.) mice, DM200 induced mice, and HSA-LR mice compared with uninduced DM5 mouse controls. (C) Western blot of protein extracts from muscle biopsies showing increased Staufen1 in DM1 patients in comparison with control individuals (anti-Staufen1; Abcam). (D) Western blot showing increased Staufen1 in muscle biopsies from additional DM1 patients compared with control biopsies and biopsies from other muscle dystrophies (anti-Staufen1; Abcam; Table S1). (E and F) Quantification of Staufen1 level in DM1 mouse models (E) and in human DM1 biopsies (F). As Staufen1 is not detected in control samples, Staufen1 levels are expressed over background. All samples from C and D were included in the quantification in F. Data are means ± SEM. **, $P < 0.01$; ***, $P < 0.001$ (Student's *t* test).

Staufen1 interacts with DMPK 3′UTR

Given that Staufen1 is known to interact with double-stranded mRNA structures through double-stranded RNA-binding domains (dsRBDs; Wickham et al., 1999) and because the CUG expansion is highly structured (Michalowski et al., 1999; Tian et al., 2000), we hypothesized that Staufen1 may directly interact with CUG-containing DMPK mRNA. We performed RNA immunoprecipitation experiments with cultured myogenic C2C12 cells transfected with plasmids encoding HA-tagged Staufen1 and a human DMPK containing 11 or 86 CTG repeats in the 3′UTR region. After formaldehyde cross-linking and Staufen1 immunoprecipitation, coimmunoprecipitated mRNAs were analyzed by quantitative RT-PCR (qRT-PCR; Fig. 2 A). Although some ectopic DMPK mRNA is recovered in the unbound fraction (unpublished data), our results clearly show that in myogenic C2C12 cells, Staufen1 does indeed interact with a subset of DMPK mRNA containing 11 and 86 CUG repeats and not with the control glyceraldehyde 3-phosphate dehydrogenase (GAPDH) mRNA.

To confirm direct binding, we performed RNA gel shift experiments with recombinant GST-Staufen1 protein and ^{32}P-radiolabeled RNA probes corresponding to the DMPK 3′UTR containing either 5 or 200 CUG repeats (Fig. 2 B). Incubation of probes with Staufen1 induces the formation of a slower migrating complex. It further reveals that Staufen1 interacts with RNA probes containing either 5 or 200 CUG repeats, whereas control GST protein did not. Importantly, the addition of an unlabeled probe as a competitor completely prevented the interaction, thereby highlighting the specificity of the interaction.

Finally, to determine whether Staufen1 binds to the CUG repeats and whether this binding is dependent of the number of repeats, we performed filter binding assays (Fig. 2 C). RNA probes containing 0, 5, 11, 40, 86, and 200 CUG repeats along with 19 and 23 nucleotides of the flanking DMPK 3′UTR sequence were generated. α-[^{32}P]ATP was used to ensure equal labeling of the probes. Our results show that recombinant Staufen1 protein interacts weakly and with similar affinity with probes containing 0, 5, or 11 CUG repeats. Remarkably, more Staufen1 proteins are necessary to saturate probes containing 40, 86, and 200 CUG repeats, indicating that more Staufen1 proteins will bind to the structure formed by the CUG^{exp} mRNA. Moreover, the increase in Staufen1 recruitment is proportional to the number of CUG repeats. Together, these results demonstrate that both in vitro and in myogenic cells, the RNA-binding protein Staufen1 is able to interact with the DMPK mRNA and that Staufen1 binds to CUG^{exp} mRNA in a length-dependent manner.

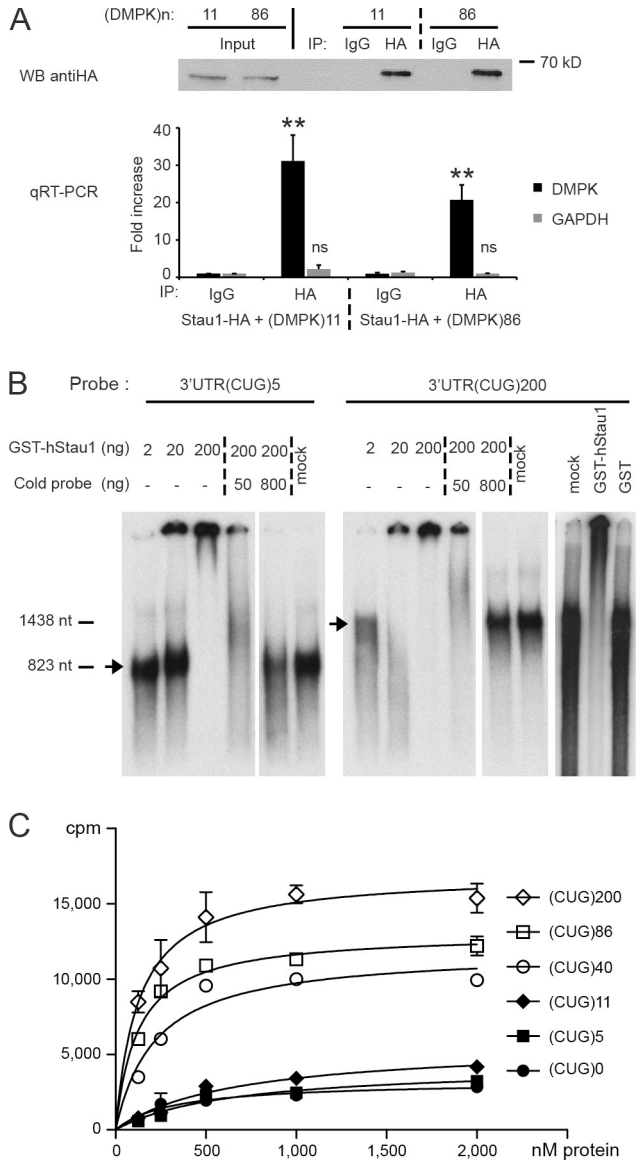

Figure 2. **Staufen1 interacts with the 3′UTR of DMPK in vitro and in vivo.** (A) RNA immunoprecipitation (IP) experiments between Staufen1 (Stau1) and DMPK mRNA. C2C12 cells were cotransfected with constructs encoding Staufen1-HA and DMPK(11) or DMPK(86). Staufen1-HA immunoprecipitation was verified by Western blotting (WB) with the anti-HA antibody, and the presence of DMPK or GAPDH mRNAs in the immunoprecipitate was determined by qRT-PCR. An anti-IgG antibody was used as a control. Absence of mRNA contamination in the wash fraction was also verified (not depicted). (B) Representative gel shift assay using ^{32}P-labeled RNA probes for the DMPK 3′UTR containing 5 or 200 CUG repeats (black arrows) incubated with increasing amounts of recombinant GST-Staufen1 protein. The specificity of the interaction was verified by adding increasing amounts of a cold probe. As additional controls, probes were incubated with BSA (mock) or GST (right). (C) Filter binding assay with ^{32}P-labeled RNA probes containing CUG repeats (0, 5, 11, 40, 86, or 200 CUG repeats) incubated with increasing amounts of Staufen1 recombinant protein. The data are means ± SEM, $n = 3$. **, $P < 0.01$ (Student's t test).

Staufen1 is not stably recruited by RNA foci

As Staufen1 can interact with DMPK 3′UTR, we wondered whether it colocalizes with nuclear aggregates of CUG^{exp} mRNAs in cells. For that purpose, we performed immunofluorescence and RNA FISH on normal and DM1 myoblasts (Fig. 3). First, we looked by immunofluorescence at the overall distribution of Staufen1 protein in control myoblasts. It was previously reported in other cell types that Staufen1 has a granular cytoplasmic distribution and nuclear exclusion, associated with a weak nucleolar staining (Marión et al., 1999; Wickham et al., 1999; Le et al., 2000; Martel et al., 2006). Here, in control myoblasts, we observed a granular distribution of Staufen1 protein in both the cytoplasm and the nucleus, along with a strong nucleolar staining. Immunofluorescence experiments revealed that the overall distribution of Staufen1 is similar in both control and DM1 myoblasts. Furthermore, the presence of nuclear Staufen1 in DM1 myoblasts does not exclusively coincide with CUG^{exp} ribonuclear foci or MBNL1 aggregates in the nucleus. Although these experiments do not exclude the possibility of a dynamic transient interaction, we conclude that Staufen1 is not stably recruited to these CUG^{exp} mRNA foci.

Staufen1 does not affect ribonuclear foci formation or MBNL1 sequestration

It is now well established that DM1 symptoms can be reversed by either reducing the level of nuclear CUG^{exp} transcripts or by competing with the sequestration of RNA-binding proteins, such as MBNL1 (Wheeler et al., 2009; François et al., 2011; Magaña and Cisneros, 2011). To determine whether Staufen1 affects CUG^{exp} aggregation and MBNL1 sequestration, two hallmarks of DM1, we analyzed ribonuclear formation by RNA FISH and MBNL1 distribution by immunofluorescence. First, C2C12 myoblasts were transfected with a GFP gene fused to the 3′UTR of DMPK carrying 200 repeats (GFP-CUG200; Amack and Mahadevan, 2001). Transfected cells displayed CUG^{exp} ribonuclear foci (Fig. 4 A) and MBNL1 sequestration (Fig. 4 B). Coexpression of Staufen1 did not prevent RNA foci formation or MBNL1 sequestration.

In a similar experiment, we assessed CUG^{exp} sequestration and MBNL1 aggregation in human DM1 myoblasts. Cultured DM1 myoblasts were transduced with a control GFP lentivirus or a Staufen1 lentivirus. Our results show that overexpression of Staufen1 in DM1 myoblasts did not decrease the number of CUG^{exp} mRNA foci (Fig. 4 C) and did not displace MBNL1 protein from nuclear aggregates (Fig. 4 D). Altogether, these results indicate that Staufen1 does not prevent or disrupt ribonuclear foci formation nor does it displace MBNL1 from CUG^{exp} mRNA aggregates.

Staufen1 rescues the nuclear–cytoplasmic export and translation of CUG^{exp} mRNA

To gain additional insight into the role of Staufen1 in DM1, we used a GFP reporter system to further assess the level of sequestration of CUG^{exp} mRNA. A similar assay has previously been used to show that hnRNP H inhibits nuclear export of CUG^{exp} (Kim et al., 2005a). C2C12 myoblasts were transfected with a GFP gene fused to the 3′UTR of DMPK carrying 5 or 200 repeats (GFP-CUG5 and GFP-CUG200, respectively; Fig. 5 A), and the level of GFP expression was assessed by immunofluorescence. Transfection of the GFP-CUG5 control construct resulted in strong GFP protein expression, indicating that transcripts containing only five CUG repeats are readily exported in

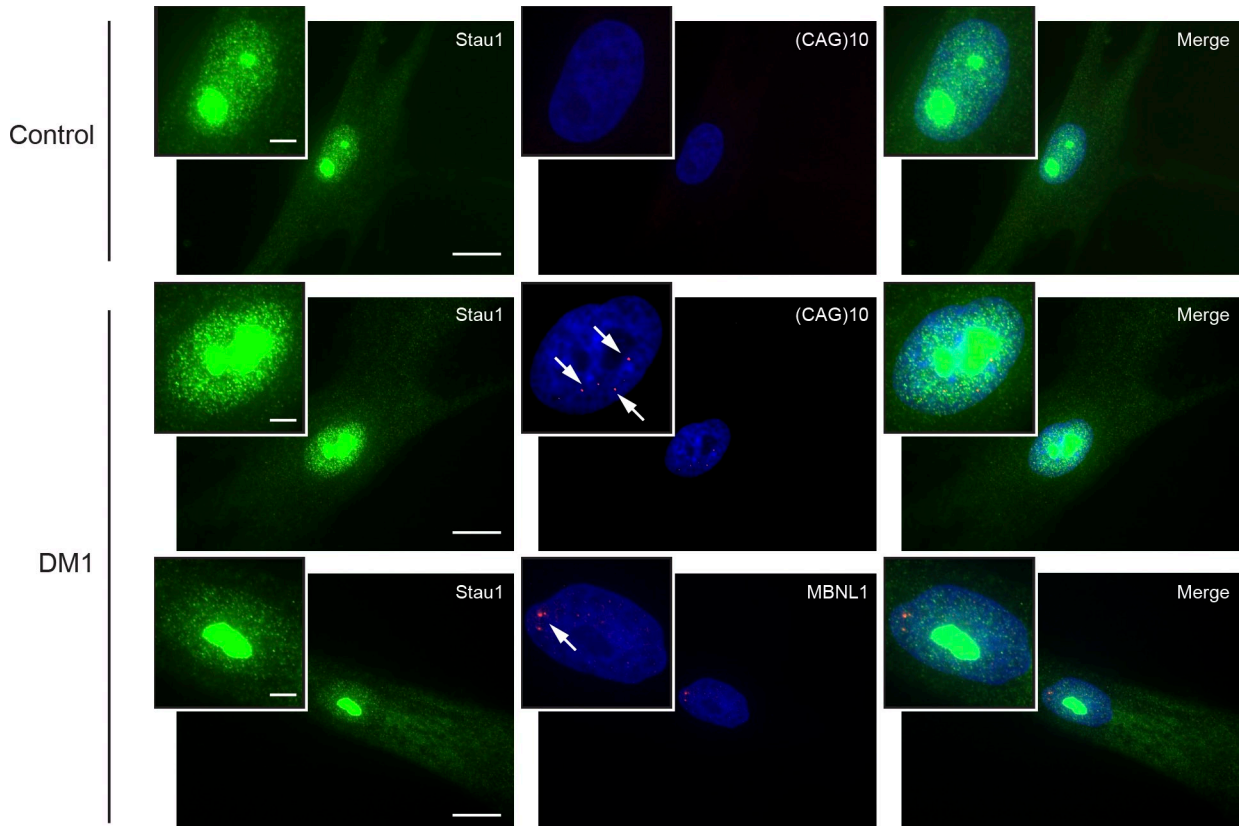

Figure 3. **Staufen1 is not sequestered by CUG^{exp} nuclear aggregates in vivo.** RNA FISH and immunofluorescence on control and DM1 myoblasts for Staufen1 (Stau1; green) and MBNL1 (red) or CUG repeats (red). Nuclei were stained with DAPI (blue). Arrows show RNA foci or MBNL1 aggregates. Insets represent higher magnifications of nuclei. Bars: (main images) 50 µm; (insets) 10 µm.

the cytoplasm and translated (Fig. 5 B). In contrast, myoblasts transfected with the GFP-CUG200 reporter plasmid resulted in lower levels of GFP expression (Fig. 5 B). This severe reduction of GFP protein expression is caused by nuclear retention of the CUG^{exp} transcript (Fig. 4 A). Remarkably, GFP-CUG200 protein expression was restored when Staufen1 was cotransfected with GFP-CUG200 (Figs. 5 B and S1). FACS measurements (Fig. 5, C and D) and Western blotting (Fig. 5 E) were also performed using these transfected cells and confirmed the rescue of GFP-CUG200 protein expression by Staufen1. In separate experiments, we determined that there was no significant difference in the abundance of GFP-CUG200 mRNAs in cells with or without Staufen1, indicating that the increase in GFP-CUG200 expression was not caused by changes in the steady-state levels of GFP-CUG200 reporter transcripts (Fig. 5 F). These results demonstrate that the RNA-binding protein Staufen1 can counteract the effect of the CUG^{exp} by enhancing the nuclear export, the cytoplasmic translation of the CUG^{exp} mRNA, or both.

The rescue of CUG^{exp} mRNA by Staufen1 takes place in mice in vivo

To assess whether the Staufen1 rescue of GFP-CUG200 protein expression also occurs in vivo, we used electroporation to create a new DM1 mouse model. Tibialis anterior (TA) muscles from WT mice were injected and electroporated with a construct containing a *Firefly Luciferase* transgene fused to the 3′UTR of *DMPK* containing 200 CTG repeats (Luc-CUG200; Fig. 6 A) to reproduce DM1 features. A *Renilla Luciferase* gene construct was coinjected to take into account the efficiency of the electroporation procedure for each muscle. 7 d after electroporation, Firefly Luciferase activity was measured and normalized to Renilla Luciferase activity (Fig. 6 B). As observed in cultured myogenic cells with GFP-CUG200, Luc-CUG200 activity was lower as compared with the control Luc-CUG5 (44.1 ± 5.9% of control values), indicating that a similar mechanism as the one observed in cultured cells (Fig. 5) takes place in vivo. Remarkably, overexpression of Staufen1 with the CUG^{exp} Luc-CUG200 construct rescued the Luciferase activity to a level close to that seen with the Luc-CUG5 control (87.0 ± 9.9%). These results show that Staufen1 can also rescue CUG^{exp} mRNA export and/or translation in a DM1 mouse model.

Rescue of the nuclear–cytoplasmic export and translation of CUG^{exp} mRNA is dependent on Staufen1 dsRBD3 and the NLS

To provide additional insights into the mechanism by which Staufen1 rescues expression of GFP-CUG200 protein, we used various Staufen1 mutant alleles. Mutations were localized in the four dsRBDs, the Tubulin-binding domain (TBD), or the NLS (Fig. 7 A).

Deletion of the TBD had no effect on the ability of Staufen1 to rescue GFP-CUG200 protein expression, indicating that mRNA transport by association with microtubules is not

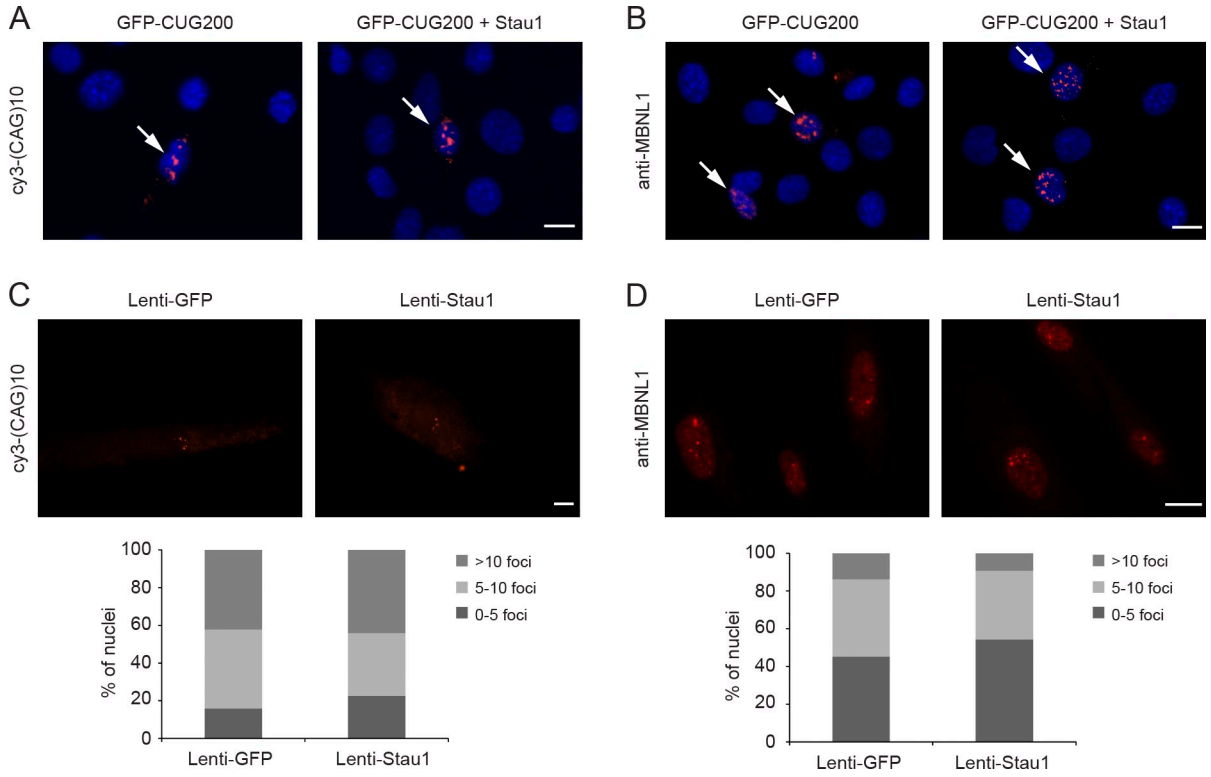

Figure 4. **Staufen1 does not modify CUG^{exp} ribonuclear foci number and MBNL1 nuclear sequestration.** (A and B) C2C12 cells were transfected with a GFP-CUG200 construct alone or cotransfected with a Staufen1 (Stau1)-HA cDNA. Cells were analyzed for CUG^{exp} ribonuclear formation (arrows) by RNA FISH with a cy3-(CAG)10 probe (A) and for MBNL1 sequestration (arrows) by immunofluorescence with an anti-MBNL1 antibody (B). (C and D) DM1 myoblasts were infected with GFP or Staufen1 lentiviruses. 1 wk after infection, distribution of CUG^{exp} ribonuclear foci (C) and MBNL1 distribution (D) were analyzed and quantified in transduced DM1 myoblasts. Bars, 50 µm.

involved in this mechanism (Fig. 7 B). Staufen1 contains four copies of dsRBD. Mutants deleted in dsRBD2 or dsRBD5 were still capable of rescuing GFP-CUG200 protein expression as expected (Fig. 7 B) because these dsRBDs were reported as nonfunctional for RNA-binding activity (Wickham et al., 1999). Although these domains have been involved in Staufen1 self-association (Martel et al., 2010), single deletion of dsRBD2 or dsRBD5 might not affect this function. In contrast, deletion and point mutation of dsRBD3 totally abolished the GFP-CUG200 protein expression rescue, whereas mutation in dsRBD4 did not, indicating that dsRBD3 is essential and functions as the major domain involved in Staufen1–DMPK mRNA interaction (Fig. 7 B). The slight variations observed in Staufen1 mutant expression levels (Fig. 7 B; Buj-Bello et al., 2002) did not affect interpretation of the aforementioned results because levels as low as 10% of Staufen1 expression are sufficient for the rescue of GFP-CUG200 expression (Fig. 7 C).

In additional experiments, we also examined the role of the NLS. Inactivation of the NLS results in a cytoplasmic Staufen1 (Martel et al., 2006) that is nonetheless still capable of associating with ribosomes while also conserving its RNA-binding activity (unpublished data). Using a deletion mutant or a point mutation in the NLS, we show that the NLS of Staufen1 is crucial in rescuing expression of GFP-CUG200 (Fig. 7 B). This indicates that the rescue of GFP-CUG200 expression by Staufen1 is not strictly caused by an increase in cytoplasmic translational activity. These findings rather suggest that the RNA-binding protein Staufen1 can counteract the effect of the CUG^{exp} by also enhancing nuclear–cytoplasmic export of the CUG^{exp} mRNA.

Staufen1 regulates alternative pre-mRNA splicing

In a separate series of experiments, we examined the functional consequences of increased Staufen1 expression in DM1 muscle (Fig. 1). Because one of the hallmarks of DM1 is aberrant splicing of key pre-mRNAs (Ranum and Cooper, 2006), we used a model system previously described with the IR and chloride channel (ClC-1) minigenes as reporters (Savkur et al., 2001; Charlet-B et al., 2002) to (a) reproduce the splicing defects induced by expression of CUG^{exp} mRNAs and (b) determine whether Staufen1 affects alternative splicing.

In DM1 cells, exon 11 of the human IR gene is preferentially skipped, resulting in a reduced cellular responsiveness to the metabolic effect of insulin (Savkur et al., 2001). In our assays, C2C12 mouse myoblasts were transfected with the IR minigene (Fig. 8 A), and the relative levels of IR-A mRNA versus IR-B mRNA were measured by RT-PCR (Fig. 8 B). In myogenic cells, the basal level of exon 11 inclusion was established at 40.4 ± 0.6%. Overexpression of a GFP-CUG200 reproduced the DM1 phenotype because it led to increased skipping of exon 11 (23.6 ± 0.5% IR-B). These levels of IR splicing using this model system are similar to ratios previously observed by others (Savkur et al., 2001). Overexpression of

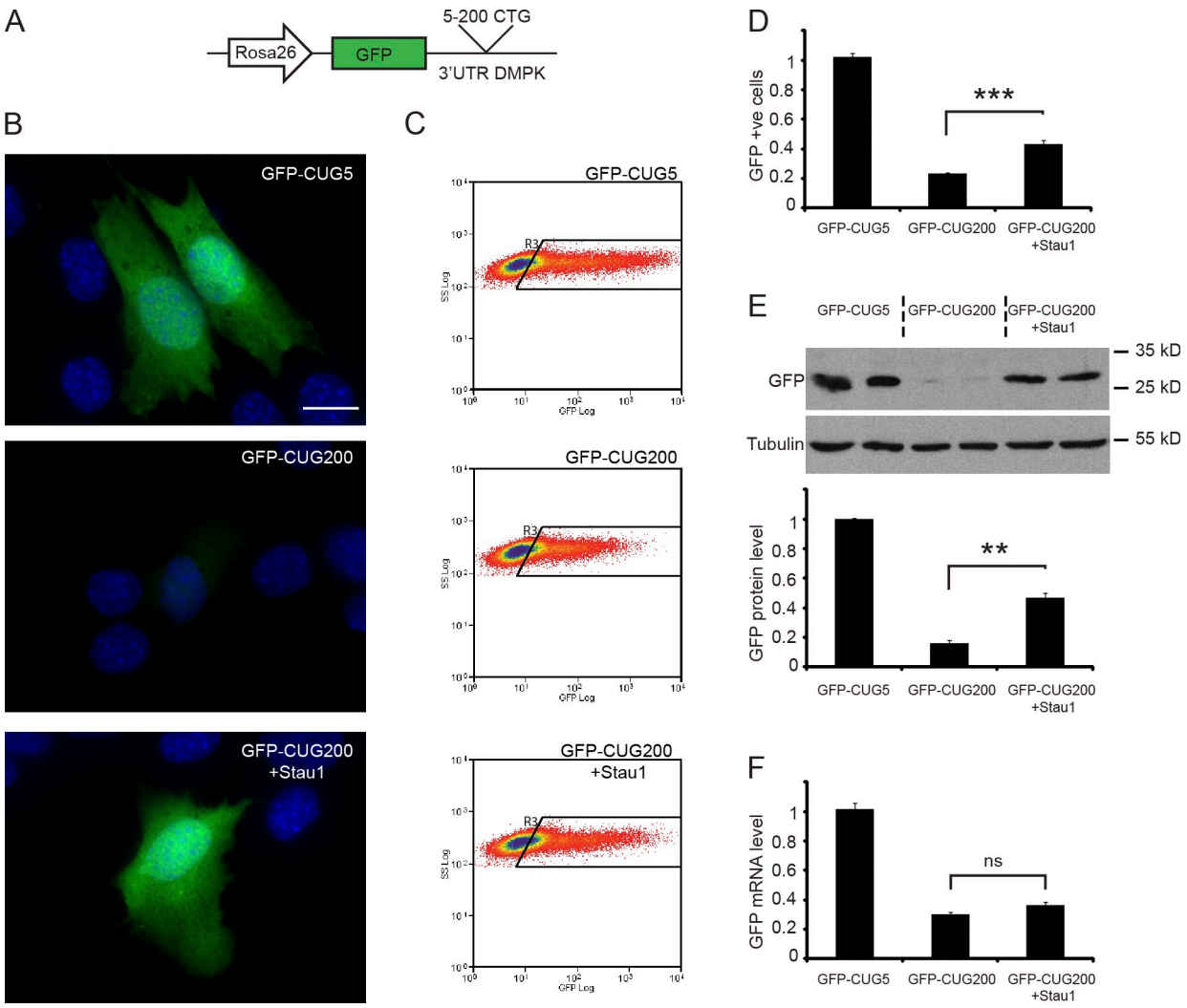

Figure 5. **Staufen1 rescues GFP-CUG200 protein expression.** (A) Schematic representation of the GFP-CUG5 and GFP-CUG200 transgenes. (B) C2C12 cells were transfected with GFP-CUG5 or GFP-CUG200 reporter plasmids alone or with the Staufen1 (Stau1) construct. Cells were fixed and analyzed by fluorescent microscopy. GFP, green; DAPI, blue. Bar, 50 µm. (C and D) GFP levels of individual cells were measured by FACS analysis. Representative FACS measurements of GFP fluorescence (GFP-positive [+ve] cells in R3 box). Data are means ± SEM, $n = 3$. (E, top) Global GFP protein levels from transfected cells were also analyzed by Western blotting using anti-GFP antibodies. Tubulin was used as a loading control. (bottom) Quantification of GFP from Western blotting. Data are means ± SEM, $n = 4$. (F) Global GFP RNA levels were analyzed by qRT-PCR quantification using primers specific for GFP. Cyclophilin B was used to normalize the data. No difference in mRNA levels was detected between GFP-CUG200 with and without the presence of Staufen1. Data are means ± SEM, $n = 4$. **, $P < 0.01$; ***, $P < 0.001$; ns, $P > 0.05$ (Student's *t* test).

Staufen1 (Fig. S1) in the presence of GFP-CUG200 completely rescued the aberrant splicing solely induced by the CUG^{exp} mRNA to a level similar to that seen in the control (45.1 ± 0.7%). This remarkable effect is not a consequence of differential stability of alternatively spliced transcripts because both exhibit a similar half-life in the presence or absence of Staufen1 (Fig. S2). Interestingly, Staufen1 overexpression alone resulted in a modest but significant switch favoring IR exon 11 inclusion (Fig. 8 B).

To confirm the role of Staufen1 in pre-mRNA splicing regulation, cultured DM1 myoblasts were transduced with lentivirus particles, and alternative splicing of endogenous IR pre-mRNA was assessed by RT-PCR (Fig. 8 D). A control GFP lentivirus established the basal level of exon 11 inclusion in these cells. As expected, overexpression of MBNL1 increased exon 11 inclusion, whereas overexpression of CUGBP1 slightly decreased it. Overexpression of Staufen1 remarkably increased inclusion of exon 11 to a level similar to that seen with MBNL1 (Fig. 8 D), thereby confirming our data obtained with the IR minigene system in C2C12 myoblasts (Fig. 8 B).

Retention of ClC-1 intron 2 results in loss of ClC-1 protein expression and a concomitant reduction in chloride conductance, causing myotonia (Mankodi et al., 2002). Albeit more modestly, we were able to extend our results to intron 2 retention of the ClC-1 minigene, indicating that the effect of Staufen1 on splicing is not limited to IR (Fig. S3). Collectively, these results establish a new role for Staufen1 in alternative splicing regulation and show that Staufen1 can reverse the effect of the CUG^{exp} mRNA on alternative splicing of key pre-mRNAs misregulated in DM1.

Staufen1 directly binds to IR pre-mRNA

Changes in MBNL1 (Miller et al., 2000; Kanadia et al., 2003) and CUGBP1 (Savkur et al., 2001; Timchenko et al., 2004;

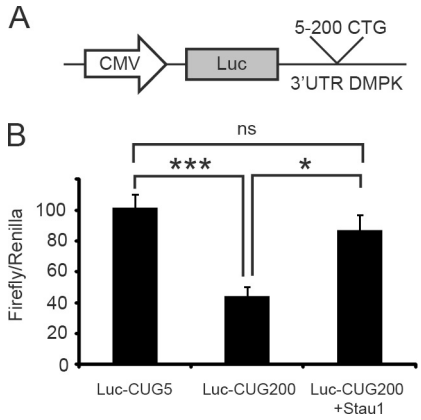

Figure 6. **Staufen1 rescues Luc200 protein expression in vivo.** (A) Schematic representation of *Firefly Luciferase* transgene with the 3′UTR DMPK containing 5 (Luc-CUG5) or 200 repeats (Luc-CUG200). (B) Mouse TA muscles were electroporated with Luc-CUG5 or Luc-CUG200 alone or with the Staufen1 (Stau1) construct. A cytomegalovirus (CMV) *Renilla Luciferase* construct was coinjected to normalize for the efficiency of the electroporation procedure. 7 d after electroporation, TA muscles were harvested, and levels of Firefly and Renilla Luciferase activity were assayed. The data are means ± SEM, $n = 12$. *, $P < 0.05$; ***, $P < 0.001$; ns, $P > 0.05$ (Student's *t* test).

Ho et al., 2005) protein activity are known to be a central mechanism in the splicing abnormalities seen in DM1. To determine whether the effect of Staufen1 on alternative splicing is caused, at least partially, by changes in the steady-state levels of CUGBP1 or MBNL1, we measured by Western blotting the level of these splicing factors in cells overexpressing Staufen1 (Fig. 8 C). Although some experiments have reported an increased level of CUGBP1 as a result of CUG^{exp} expression (Jones et al., 2011), we did not detect such an increase under our conditions. Nevertheless, our results showed that transfection of Staufen1 cDNA in C2C12 myoblasts had no effect on endogenous MBNL1 and CUGBP1 expression, indicating that Staufen1 overexpression does not affect the level of key splicing regulators (Fig. 8 C).

To gain additional insights into the mechanism involved in Staufen1-regulated splicing, we also tested the possibility of an interaction between Staufen1, CUGBP1, and MBNL1 by coimmunoprecipitation experiments. This appeared particularly important because an interaction between hnRNP H, CUGBP1, and MBNL1 has been shown to regulate IR splicing in normal and DM1 myoblasts (Paul et al., 2006). Therefore, plasmids expressing Staufen1-HA and MBNL1-myc or CUGBP1-myc were cotransfected in C2C12 myoblasts (Fig. 8 E). Staufen1 protein was immunoprecipitated with an anti-HA antibody, and coimmunoprecipitated proteins were analyzed by Western blotting. Although we were able to confirm the known interaction between Staufen1-HA and endogenous Upf1 protein (Kim et al., 2005b), used here as a positive control, no MBNL1 or CUGBP1 proteins appeared coimmunoprecipitated, thereby indicating an absence of interaction between Staufen1 and MBNL1 or CUGBP1 (Fig. 8 E).

Finally, we hypothesized that Staufen1 may directly interact with secondary structures present in the IR pre-mRNA. This appeared as an attractive hypothesis because it has recently been shown that MBNL1 can regulate alternative splicing via direct interaction with pre-mRNAs (Ho et al., 2004; Warf and Berglund, 2007; Yuan et al., 2007; Warf et al., 2009). Therefore, we performed RNA immunoprecipitation experiments with cultured myogenic C2C12 cells transfected with HA-tagged Staufen1 cDNA and the IR minigene. After immunoprecipitation of Staufen1 with anti-HA antibodies, coimmunoprecipitated RNAs were analyzed by qRT-PCR using primers specific for the IR intronic sequence (Fig. 8 F). Our results clearly show that in myogenic C2C12 cells, Staufen1 interacts with IR pre-mRNA and not with the control GAPDH mRNA (Fig. 8 E). We therefore hypothesize that regulation of alternative splicing by Staufen1 can take place through a direct interaction of Staufen1 with pre-mRNAs. Altogether, our results describe Staufen1 as a new alternative splicing regulator and show that regulation of its level in DM1 can rescue a major hallmark of the pathology.

Discussion

DM1 is caused by an expansion of CUG repeats in the 3′UTR of the DMPK mRNA. The CUG^{exp} mRNA becomes toxic to cells by affecting RNA metabolism through the deregulation of RNA-binding proteins. In the past decade, two proteins have been intensely studied and have been proposed to play a major role in the DM1 pathology, namely MBNL1 and CUGBP1 (Ranum and Cooper, 2006; Wheeler and Thornton, 2007; Lee and Cooper, 2009; O'Rourke and Swanson, 2009; Schoser and Timchenko, 2010). Here, we show for the first time that the RNA-binding protein Staufen1 is misregulated in DM1 skeletal muscle and uncover a new role for Staufen1 in regulation of alternative splicing.

In this work, we show that the level of the RNA-binding protein Staufen1 is markedly and specifically elevated in DM1 skeletal muscle. The increase in Staufen1 expression is seen in biopsies from patients with adult-onset DM1 as well as in three different DM1 mouse models but not in other types of dystrophies, such as DMD and X-linked myopathy. Over the last few years, expression of some RNA-binding proteins was shown to be increased in DM1 skeletal muscle as a result of the CUG^{exp} RNA expression. CUGBP1 was the first RNA-binding protein discovered to be up-regulated in DM1 muscles (Savkur et al., 2001), and accordingly, mice overexpressing CUGBP1 display symptoms and splicing abnormalities seen in the DM1 pathology (Timchenko et al., 2004; Ho et al., 2005). More recently, the hnRNP H protein was also shown to be increased in response to CUG^{exp} mRNA, and its impact on DM1 is similar to that of CUGBP1 (Kim et al., 2005a; Paul et al., 2006). Although the mechanisms leading to the up-regulation of these RNA-binding proteins is not fully understood, it was recently shown that the CUGBP1 up-regulation is mediated through a PKC signaling-dependent phosphorylation event, leading to increased protein stabilization (Kuyumcu-Martinez et al., 2007). There is currently no information concerning the nature of the mechanisms regulating expression of Staufen1 in skeletal muscle fibers in vivo. Hence, the discovery of a pathological condition in which Staufen1 levels are affected represents a unique opportunity to begin dissecting the regulatory

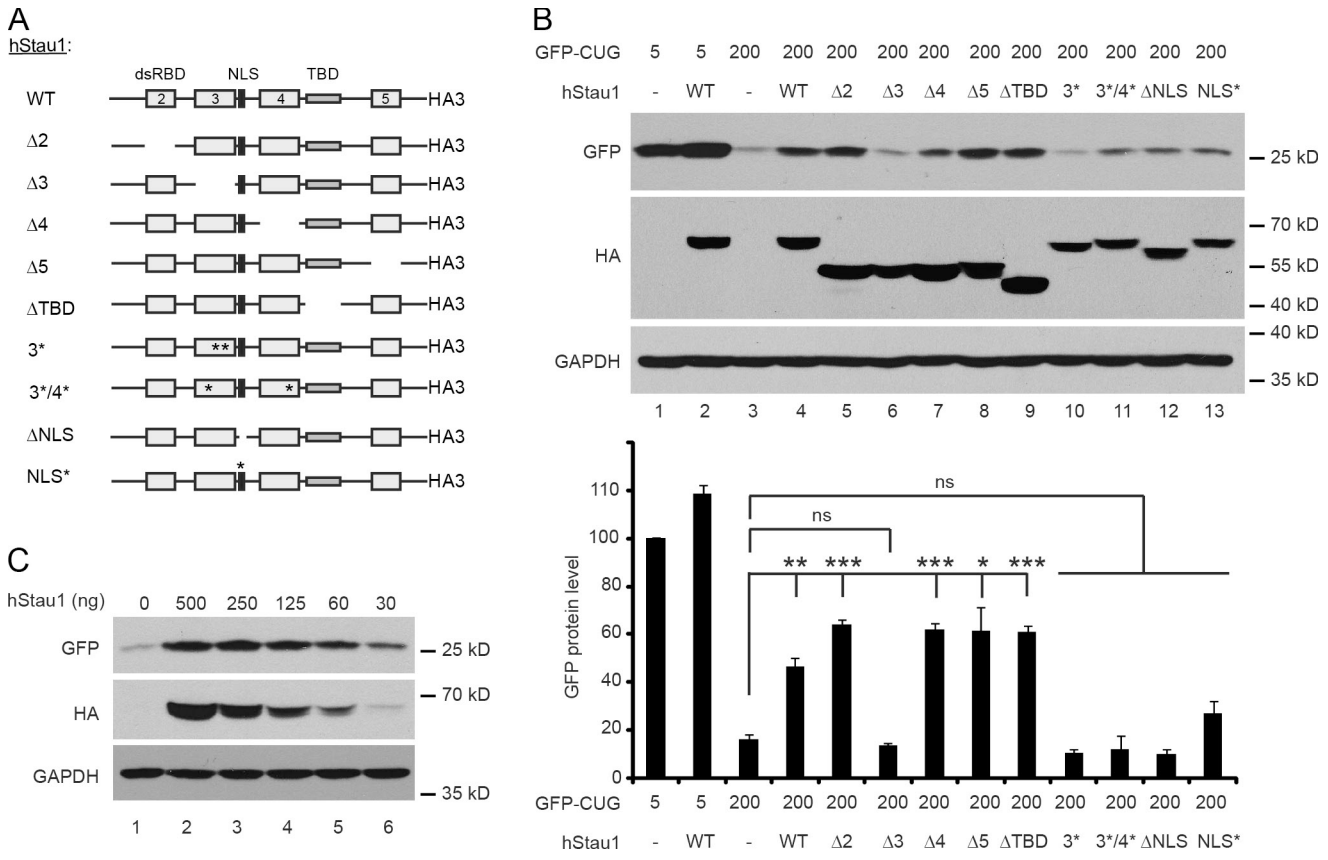

Figure 7. **The dsRBD3 and NLS are essential domains for the Staufen1 rescue of GFP-CUG200 protein expression.** (A) Schematic representation of Staufen1 (Stau1) mutants used in these experiments. (B) C2C12 cells were transfected with GFP-CUG5 or GFP-CUG200 reporter plasmids alone or with the various Staufen1 constructs. (top) GFP protein levels were determined by Western blotting using anti-GFP antibodies. The anti-HA antibody was used to show expression of Staufen1 mutants. GAPDH was used as a loading control. (bottom) Quantifications of GFP protein levels from transfected cells as determined by Western blotting. The data are means ± SEM, $n = 4$. (C) C2C12 cells were transfected with GFP-CUG200 reporter plasmid alone or cotransfected with decreasing amounts of the Staufen1 construct. GFP protein levels were analyzed by Western blotting using anti-GFP antibodies. The anti-HA antibody was used to show the expression level of Staufen1. GAPDH was used as a loading control. *, $P < 0.05$; **, $P < 0.01$; ***, $P < 0.001$ (Student's *t* test).

events presiding over the expression of Staufen1. In this context, it will be interesting to determine whether a common signaling pathway controls expression of CUGBP1, hnRNP H, and Staufen1 in the DM1 pathology.

The role of CUGBP1 in DM1 was originally identified through its ability to bind CUG repeats (Timchenko et al., 1996). Subsequently, MBNL1 was also shown to interact with CUG expansions in the context of DM1 (Miller et al., 2000). Because Staufen1 is known to associate with double-stranded RNA secondary structures and because CUG expansion forms a large secondary structure, we hypothesized that Staufen1 may interact with CUG repeats. Using in vivo and in vitro complementary approaches, we show that, indeed, the RNA-binding protein Staufen1 directly interacts with the 3′UTR of DMPK mRNA. Remarkably, more Staufen1 proteins can bind to the expanded CUG repeats. However, similar to CUGBP1, Staufen1 is not sequestered by nuclear aggregates of CUG^{exp} mRNAs.

We uncovered a novel function of Staufen1 in the regulation of alternative pre-mRNA splicing. These findings are exciting because one of the hallmarks of the DM1 pathology is the aberrant pre-mRNA splicing that results from an alteration in the abundance of RNA-binding proteins. The aforementioned two main RNA-binding proteins associated so far with DM1, CUGBP1, and MBNL1 have previously been shown to be key splicing regulators with antagonistic impacts especially on IR splicing. Thus, the CUGBP1 increase (Savkur et al., 2001) and the decreased MBNL1 functional availability caused by the CUG^{exp} mRNA (Miller et al., 2000) both result in a coordinated deleterious effect toward skipping of the IR exon 11, thereby leading to the expression of a lower affinity receptor. In our work, we show that Staufen1 is also an alternative splicing regulator but, importantly, acts toward inclusion of IR exon 11. One can thus envisage a model in which Staufen1 counterbalances the combined negative effect of CUGBP1 and MBNL1 on splicing, which could clearly be of benefit in DM1. One could speculate that without this increase in Staufen1 expression, the DM1 pathology may be even more severe for a given number of CTG repeats.

We initiated several series of experiments to begin gaining insights into the mechanisms by which Staufen1 regulates alternative splicing. Here, we show that the increase in Staufen1 does not affect the expression of MBNL1 and CUGBP1 in myogenic cells. Moreover, we did not detect any interaction between Staufen1 and MBNL1 or between Staufen1 and CUGBP1. However, we show a direct interaction of Staufen1 with IR pre-mRNAs. One may thus think that Staufen1 regulates alternative

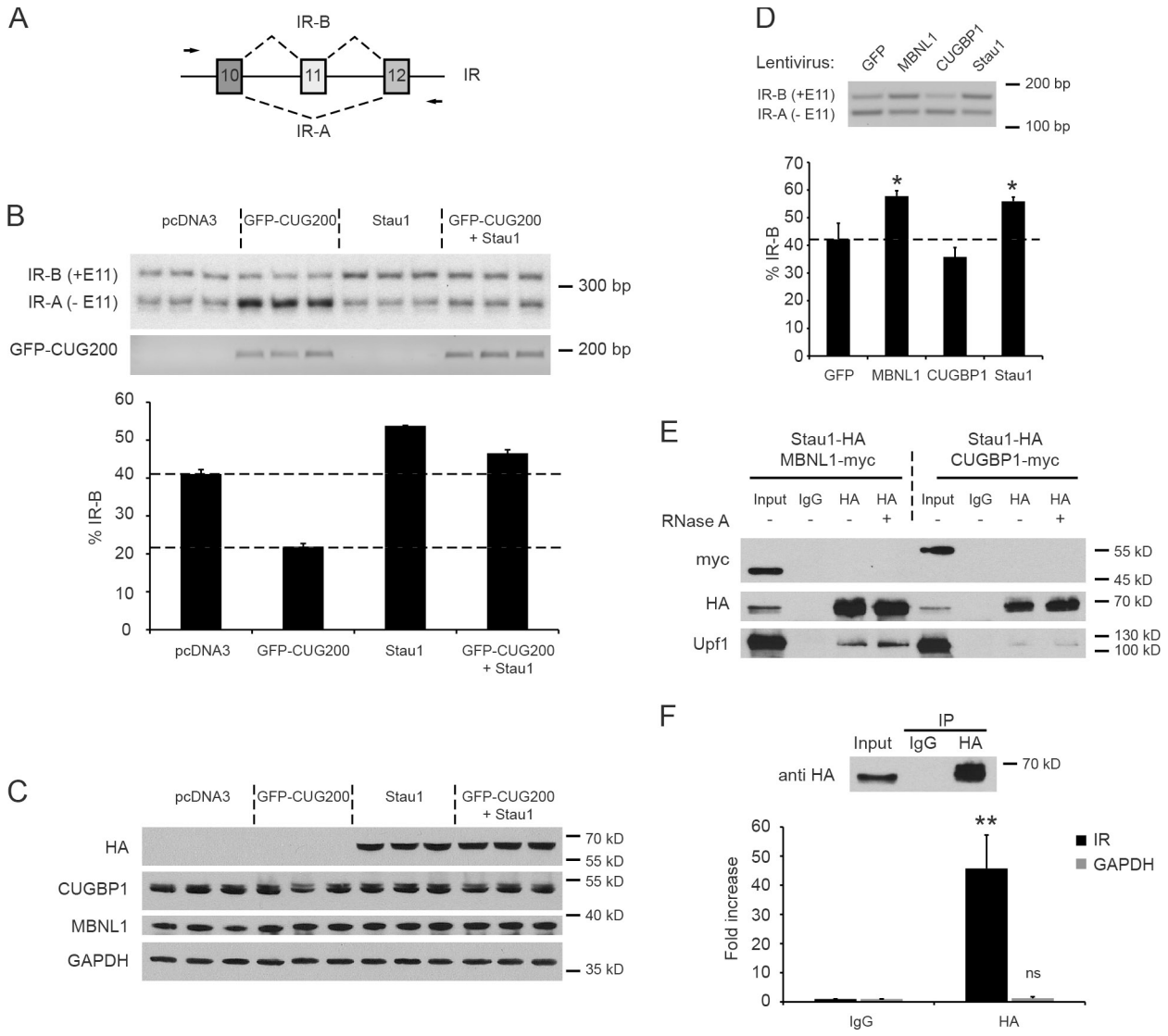

Figure 8. **Staufen1 regulates IR alternative splicing.** (A) Representation of the *insulin receptor* (*IR*) minigene. (B) C2C12 cells were transfected with the IR minigene and cotransfected with constructs expressing GFP-CUG200 and/or Staufen1 (Stau1)-HA. (top) Alternative splicing of the IR minigene was analyzed by RT-PCR using ^{32}P-labeled primers followed by electrophoresis in a 5% polyacrylamide gel and autoradiography. The size of PCR products was confirmed by agarose gel electrophoresis. (bottom) Quantification of the splicing was performed by expressing the amount of the IR-B over the total (IR-A plus IR-B). Dotted lines represent the percentage of IR-B splicing in pcDNA3 control and GFP-CUG200–transfected cells. Note that addition of Staufen1 rescues the splicing pattern toward that seen with the control plasmid (pcDNA3) despite the presence of GFP-CUG200. (C) C2C12 cells were transfected as in B, and levels of RNA-binding proteins were analyzed by Western blotting. (D) DM1 myoblasts were transduced with GFP, MBNL1, CUGBP1, or Staufen1 lentivirus particles. Alternative splicing of endogenous IR was analyzed by RT-PCR. The dotted line represents the percentage of IR-B splicing in GFP control. (E) Representative coimmunoprecipitation experiment. C2C12 cells were transfected with constructs expressing Staufen1-HA and CUGBP1-myc or MBNL1-myc. Immunoprecipitated proteins were analyzed by Western blotting. (F) RNA immunoprecipitation (IP) experiment between Staufen1 and IR pre-mRNA. C2C12 cells were cotransfected with constructs encoding Staufen1-HA and IR minigene. Staufen1-HA immunoprecipitation was verified by Western blotting with anti-HA antibody, and the presence of coimmunoprecipitated IR pre-mRNA or GAPDH mRNAs was determined by qRT-PCR. An anti-IgG antibody was used as a control. Data are means ± SEM, $n = 3$. *, $P < 0.05$; **, $P < 0.01$.

splicing by direct binding to pre-mRNAs. Additional work will be necessary to identify the Staufen1 binding sites in the pre-mRNA and determine whether Staufen1 competes with MBNL1 binding sites.

A direct effect of CUG expansion is the retention and accumulation of CUG^{exp} mRNAs in the nucleus. This nuclear retention prevents CUG^{exp} mRNAs from being efficiently exported into the cytoplasm and translated. It is known that DM1 symptoms can be reversed by reducing the levels of nuclear CUG^{exp} transcripts (Wheeler et al., 2009). As nuclear aggregation of mRNA and mRNA transport into the cytoplasm are two competing events within the nucleus, the rescue of GFP or Luciferase protein expression by Staufen1 seen in our experiments reflects a decrease of nuclear retention of the CUG^{exp} mRNA with subsequent translation. The fact that a cytoplasmic Staufen1, achieved via NLS mutations, does not rescue expression of the GFP-CUG200 construct rules out a simple increase of translation by Staufen1 and suggests, instead, that the increase in GFP protein level also involves an increased export of CUG^{exp} mRNA. However, no difference in GFP-CUG200 mRNA subcellular

localization was observed by RNA FISH or cell fractionation (Fig. S4). The reason for this discrepancy is unclear but may suggest that the GFP reporter assay used in our experiments is very sensitive and can detect increases in mRNA export and translation that cannot be easily monitored by RNA FISH or fractionation experiments. Nonetheless, our results thus suggest that the increase in Staufen1 may be sufficient to promote the transport of more CUG^{exp} mRNA out of the nucleus. The fact that no major difference was noticed in CUG^{exp} foci number and GFP mRNA localization in the presence of an increased level of Staufen1 suggests that Staufen1 might interact with either existing CUG^{exp} released from mRNA aggregates or from neosynthesized transcripts, because it is known that CUG^{exp} aggregates are labile structures constantly forming and disaggregating (Querido et al., 2011).

Both MBNL1 and CUGBP1 are known to assume more functions in addition to their roles as splicing regulators. For example, CUGBP1 modulates translation and mRNA stability (Timchenko et al., 2001, 2004), whereas MBNL1 modulates micro-RNA biogenesis (Rau et al., 2011). Because DM1 is a complex disorder, it appears plausible, therefore, that misregulation of MBNL1 and CUGBP1 can also perturb these distinct functional roles, causing additional molecular events to occur aberrantly in DM1 cells along with missplicing. Staufen1 is also well recognized as a multifunctional protein known to regulate mRNA transport (Kiebler et al., 1999), translation (Dugré-Brisson et al., 2005), and stability of transcripts (Kim et al., 2005b, 2007). Thus, it is also possible that Staufen1 can compensate not only for splicing defects in DM1 but that it may also positively impact several other disease mechanisms yet to be fully characterized. Our discovery of the involvement of another multifunctional RNA-binding protein in DM1 and of its new role in splicing adds an additional layer of complexity in the etiology of the DM1 pathology.

Given our findings showing that Staufen1 rescues two hallmarks of the DM1 pathology, namely aberrant splicing of pre-mRNAs and nuclear export/translation of CUG^{exp} transcripts, which are both expected to cause beneficial effects in the DM1 context, we propose that Staufen1 up-regulation observed in skeletal muscle from mouse models and DM1 patients may thus serve a protective role in the DM1 pathology. Collectively, it appears reasonable to suggest that the increase in Staufen1 may indeed be a compensatory mechanism used by muscle fibers to reduce and/or delay the detrimental effects caused by MBNL1 sequestration and CUGBP1 up-regulation. If this hypothesis is confirmed, regulation of Staufen1 levels could therefore represent a novel therapeutic avenue for developing treatments for DM1.

Materials and methods

Constructs and antibodies

The constructs used in this study were pcDNA3 (Invitrogen), GFP-CUG5, GFP-CUG200 (Amack and Mahadevan, 2001), hStaufen1^{55}-HA_3 (Wickham et al., 1999), hStaufen1^{55}-Δ2-HA_3, hStaufen1^{55}-Δ3-HA_3, hStaufen1^{55}-Δ4-HA_3, hStaufen1^{55}-Δ5-HA_3, hStaufen1^{55}-ΔTBD-HA_3 (Luo et al., 2002), hStaufen1^{55}-3*-HA_3, hStaufen1^{55}-3*/4*-HA_3, hStaufen1^{55}-ΔNLS-HA_3, and hStaufen1^{55}-NLS*-HA_3 (Martel et al., 2006). IR-N minigene (Kosaki et al., 1998) and ClC-1 minigene (Charlet-B et al., 2002) were gifts from T. Cooper (Baylor College of Medicine, Houston, TX) and N. Webster (University of California, San Diego, La Jolla, CA). For RNA immunoprecipitation, pc-DMPK(11) and pc-DMPK(86) vectors were gifts from R. Korneluk (Children's Hospital of Eastern Ontario, Ottawa, Ontario, Canada). For gel shift experiments, DMPK 3′UTR was extracted from GFP-CUG5 and GFP-CUG200 constructs by EcoRI–XhoI digestion and subcloned in a pcDNA3 vector. For GST-hStaufen1 recombinant protein production, the hStaufen1 insert was digested by PshAI–HincII from hStaufen1-HA_3 and subcloned in frame into a blunted SalI site of pGEX-4T-1 (GE Healthcare). Luc-CUG5 and Luc-CUG200 constructs were obtained by cloning the *Luciferase* transgene from pGL4.14 (Promega) into NheI and NotI sites of pcDNA3.1 Hygro (Invitrogen) and by cloning the DMPK 3′UTR from GFP-CUG5 and GFP-CUG200 plasmids downstream of the *Luciferase* gene in the XbaI site, respectively.

For filter binding assays, pc-CUG5, pc-CUG11, pc-CUG40, pc-CUG86, and pc-CUG200 constructs were obtained from GFP-CUG5, pc-DMPK(11), pc-DMPK(40), pc-DMPK(86), and GFP-CUG200 vectors, respectively, by PCR amplification of the CUG repeat region using the following primers: forward, 5′-GGATAAGCTTGTCCTTGTAGCCGGGAATG-3′, and reverse, 5′-CCATCTCGAGAAAGAAATGGTCTGTGATCC-3′ (HindIII and XhoI restriction sites are underlined in the primer sequences). PCR products were subcloned into HindIII–XhoI sites of pcDNA3. For the pc-CUG0 construct, the pc-CUG5 construct was used as a template, and two rounds of PCR amplification were first performed with the following primers: 5′-TACATCAATGGGCGTGGATA-3′ and the flanking primer 5′-TGATCCCCCCCATTCCCGGCTACAAGGACG-3′ (reaction 1) and the flanking primer 5′-GCCGGGAATGGGGGGATCACAGACCATTT-3′ and primer 5′-GCGATGCAATTTCCTCATTT-3′ (reaction 2). To remove the internal CTG region (15 nucleotides), we performed a third round of PCR with the reaction 1 and reaction 2 PCR products using the two flanking primers listed in this paragraph to yield a product containing the DMPK 3′UTR sequence without the CTG region as confirmed by sequencing. The antibodies used in this study were anti-Staufen1 (Bélanger et al., 2003), anti-Staufen1 (Abcam), anti-GAPDH (Advanced ImmunoChemical), anti-Tubulin (Sigma-Aldrich), anti-HA.11 (Covance), anti-GFP (Roche), anti-MBNL1 (Santa Cruz Biotechnology, Inc.), anti-CUGBP1 (Santa Cruz Biotechnology, Inc.), anti-Upf1 (Millipore), and anti-myc (supernatant from hybridoma; 9E10; American Type Culture Collection).

Cell culture and transfections

Mouse C2C12 cells (American Type Culture Collection) were maintained as myoblasts in growth medium (DME, 10% fetal bovine serum [HyClone; Thermo Fisher Scientific], 100 U/ml penicillin, and 100 µg/ml streptomycin). Control and DM1 human fibroblasts (GM03377 and GM03132, respectively; Coriell Cell Repository) were cultured under the same conditions (a gift from A. MacKenzie, Children's Hospital of Eastern Ontario, Ottawa, Ontario, Canada). Cell transfections were performed with 1 µg plasmid DNA, Lipofectamine, and Plus Reagent (Invitrogen) according to the manufacturer's instructions.

MyoD conversion of DM1 fibroblasts

The pBRIT-MyoD vector (a gift from M. Rudnicki, Ottawa Hospital Research Institute, Ottawa, Ontario, Canada) was transfected in Phoenix-Ampho cells. The conditioned medium containing viral particles was collected and used to infect control and DM1 fibroblasts overnight in the presence of 4 µg/ml Polybrene (Sigma-Aldrich). The transduced cells were grown, and stable cell lines were selected for ≥2 wk in presence of 1 µg/ml puromycin. MyoD-converted fibroblasts are called DM1 myoblasts in this paper.

Lentivirus production and transduction

hStaufen1 cDNA was subcloned from hStaufen1^{55}-HA_3 into pCDH-CMV-MCS-EF1-copGFP (System Biosciences). pCDH-MBNL1 and pCDH-CUGBP1 were gifts from R. Pelletier (Center Hospital of the University of Laval Research Center, Quebec City, Quebec, Canada). pCDH-CMV-MCS-EF1-copGFP, pCDH-MBNL1, pCDH-CUGBP1, and pCDH-Staufen1 viral particles were produced by transient transfection of 293T cells with the lentiviral packaging mix (ViraPower; Invitrogen). The conditioned medium containing viral particles was collected and used to transduce control and DM1 myoblasts overnight in the presence of 4 µg/ml of Polybrene. The transduced cells were grown for several days before analyses.

Western blotting

HSA-SR and HSA-LR samples were gifts from C. Thornton (University of Rochester, Rochester, NY). Cells were washed and resuspended in radioimmunoprecipitation assay (RIPA) buffer (50 mM Tris-HCl, pH 8.0, 150 mM NaCl, 1% NP-40, 0.5% sodium deoxycholate, 0.1% SDS, and protease inhibitors [Complete; Roche]). Protein concentration was determined with a bicinchoninic acid protein assay kit (Thermo Fisher Scientific). 30 µg of

total protein was separated by SDS-PAGE and transferred onto nitrocellulose membranes. Nonspecific binding was first blocked with PBS and 0.05% Tween containing 5% skim milk, and membranes were then incubated with primary antibodies. After washing with PBS and 0.05% Tween, membranes were incubated with HRP-conjugated secondary antibodies (Jackson ImmunoResearch Laboratories, Inc.). After several washes with PBS and 0.05% Tween, signals were revealed using ECL reagents (PerkinElmer) and autoradiographed with x-ray films (Thermo Fisher Scientific). Quantifications were performed with ImageJ software (National Institutes of Health).

RNA immunoprecipitation

24 h after transfection, myoblasts were washed and fixed in 1% formaldehyde for 10 min at room temperature, and the reaction was then quenched for 10 min by incubation in PBS/0.25 M glycine. Cells were washed and resuspended in RIPA buffer. Cross-linked complexes were solubilized on ice by four 15-s sonication pulses, and the insoluble material was removed by centrifugation (16,000 *g* for 10 min at 4°C). Equivalent amounts of lysate were precleared with protein A/G plus beads (Santa Cruz Biotechnology, Inc.), 200 µg/ml of competitor tRNA, and 40 µg/ml of salmon sperm DNA. Complexes were immunoprecipitated using 3 µg of specified antibodies and protein A/G plus beads overnight at 4°C. After four washes with RIPA buffer and two washes with TE buffer (10 mM Tris-HCl, pH 8.0, and 1 mM EDTA), beads containing the immunoprecipitated samples were collected and resuspended in 100 µl of elution buffer (50 mM Tris-HCl, pH 7.0, 5 mM EDTA, 10 mM DTT, and 1% SDS). Formaldehyde-induced cross-linking was then reversed (5 h at 70°C). Aliquots were analyzed by Western blotting to determine the efficiency of immunoprecipitation. The remaining of samples was used for RNA extraction and RT-PCR analysis.

Gel shift

RNA probes were transcribed from a linearized pcDNA3 vector containing the DMPK 3′UTR templates using an in vitro transcription kit (MAXIScript; Invitrogen) according to the manufacturer's instructions. 800 Ci/mmol α-[^{32}P]ATP (PerkinElmer) was used for radiolabeling RNA probes. Unincorporated nucleotides were removed, and probes were purified by electrophoresis on 6% Tris-glycine-polyacrylamide gels. Bacterially expressed recombinant GST-hStaufen1 was affinity purified on a glutathione–Sepharose matrix (GE Healthcare) and quantified using a bicinchoninic acid kit. 2–200 ng GST-hStaufen1 protein and 12,000 cpm RNA probe were preincubated for 30 min at room temperature in SP mix (625 µM ATP, 25 mM creatine phosphate, 4 mM $MgCl_2$, 2.5 mM DTT, 3.25% polyvinyl alcohol, and 2.5 U RNase inhibitor; Coté et al., 2001). For competition experiments, nonradiolabeled RNA was added 15 min before the end of the preincubation step. Samples were separated on Tris-glycine-polyacrylamide gels using 4% acrylamide/bisacrylamide (19:1). After electrophoresis, the gels were dried and subjected to autoradiography.

Filter binding assays

Uniformly labeled RNA probes were produced from the linearized pc-CUG0, pc-CUG5, pc-CUG11, pc-CUG40, pc-CUG86, and pc-CUG200 vectors using 800 Ci/mmol α-[^{32}P]ATP and the in vitro transcription kit (MAXIScript) according to the manufacturer's instructions. Increasing concentrations of Staufen1 recombinant proteins or GST controls were incubated with 50,000 cpm (180 fmol) RNA probes in binding buffer (10 mM Tris-HCl, pH 7.4, 3 mM $MgCl_2$, 300 mM KCl, 1 mM DTT, 0.5 µg tRNA, and 5 U RNase inhibitor) at 22°C for 10 min. Each reaction was applied to the microfiltration apparatus (Bio-Dot; Bio-Rad Laboratories) containing a nitrocellulose membrane (Bio-Rad Laboratories) followed by two washes with binding buffer. Membranes were vacuum dried for 30 min, and each well was quantified using a liquid scintillation counter (1414; Wallac). Data were analyzed using the Prism 5 software (GraphPad Software) and the one-site binding model.

Immunofluorescence and RNA FISH

Cells were fixed for 15 min in 4% formaldehyde/PBS and permeabilized for 15 min with 0.5% Triton X-100 in PBS. Cells were then incubated with the primary antibodies diluted with 1% BSA in PBS for 1 h, washed in PBS, and incubated for 1 h with Alexa Fluor 488 or 594 secondary antibodies (Invitrogen). For RNA FISH, cells were placed in 40% formamide and 2× SSC for 10 min and incubated for 2 h with 10 ng Cy3-labeled (CAG)10 oligonucleotide probe in hybridization buffer (40% formamide, 2× SSC, 0.2% BSA, 10% dextran sulfate, 2 mM vanadyl adenosine complex, 1 mg/ml tRNA, and salmon sperm DNA). After washes, slides were mounted with mounting medium containing DAPI (Vectashield; Vector Laboratories). Fluorescent images were visualized by microscopy at room temperature on a microscope (Axio Imager.Z1; Carl Zeiss) equipped with EC Plan-Neofluar 40×/0.75 NA and Plan-Apochromat 63×/1.4 NA oil objective lenses (Carl Zeiss). Images were acquired with a camera (AxioCam HRm; Carl Zeiss) and processed with the AxioVision software (Carl Zeiss) and Photoshop (CS5; Adobe).

RNA extraction, reverse transcription, PCR, and real-time quantitative PCR

Total RNAs were first extracted from samples using TRIZOL (Invitrogen) or TriPure (Roche). 1 ug of total RNA was DNase treated to remove contaminating DNA (DNA-free; Invitrogen). cDNAs were synthesized from DNase-treated RNAs using the reverse transcriptase (MuLV; Applied Biosystems). Alternative splicing of minigenes was analyzed by PCR as previously described (Savkur et al., 2001; Charlet-B et al., 2002; Cooper, 2005) using the following primers: IR forward, 5′-TAATACGACTCACTATAGGGC-3′; IR reverse, 5′-GCTGCAATAAACAAGTTCTGC-3′; ClC-1 forward, 5′-AGGGATGCCCAAGAAGACAGGCT-3′; and ClC-1 reverse, 5′-GCCATCAGCAGTCCCAGAAGCAC-3′. Endogenous IR alternative splicing was analyzed using the following primers (Savkur et al., 2001): IR forward, 5′-CCAAAGACAGACTCTCAGAT-3′, and IR reverse, 5′-AACATCGCCAAGGGACCTGC-3′. Levels of mRNA expression were then evaluated by PCR or real-time quantitative PCR (MX3005P; Agilent Technologies) using the SYBR Green PCR kit (QuantiTect; QIAGEN) according to the manufacturer's instructions. Sequences of the primers were as follows: hDMPK forward, 5′-GTTCGCCGTTGTTCTGTCTC-3′, and reverse, 5′-CCGGAGTCGAAGACAGTTCT-3′; hDMPK 3′UTR forward, 5′-CCGTTGGAAGACTGAGTGC-3′, and reverse, 5′-CATTCCCGGCTACAAGGAC-3′; GFP forward, 5′-AGAACGGCATCAAGGTGAAC-3′, and reverse, 5′-TGCTCAGGTAGTGGTTGTCG-3′; U6 forward, 5′-CGCTTCGGCAGCACATATAC-3′, and reverse, 5′-GCTTCACGAATTTGCGTGTC-3′; Y3 forward, 5′-TTGGTCCGAGAGTAGTGGTG-3′, and reverse, 5′-AGGCTGGTCAAGTGAAGCAG-3′; GAPDH forward, 5′-GGGTGTGAACCACGAGAAAT-3′, and reverse, 5′-CCTTCCACAATGCCAAAGTT-3′; and IR intron forward, 5′-GCTCTCTTAGTGGGTGCCAAT-3′, and reverse, 5′-AAGGGCTCCATTCAGACTCC-3′. Expression levels were normalized to Cyclophilin B mRNA levels using the following primers: forward, 5′-GATGGCACAGGAGGAAAGAG-3′, and reverse, 5′-AACTTTGCCGAAAACCACAT-3′.

FACS analysis

24 h after transfection, myoblasts were briefly washed, trypsinized, strained through 50-mm mesh filters (Partec), and suspended at a concentration of 1–4 × 10^6 cells/ml. Cells were separated on a cytometer (MoFlo; Dako) equipped with three lasers. Acquisition gates for GFP measurements were strictly defined based on untransfected control cells as well as the GFP-transfected positive control.

In vivo electroporation

Surgical procedures were performed using aseptic techniques and in complete agreement with the University of Ottawa Animal Care and Use Committee in compliance with the Guidelines of the Canadian Council on Animal Care and the Animals for Research Act. 5-wk-old C57BL/6 female mice were anaesthetized by isoflurane inhalation. A 30-µl volume of 0.9% NaCl containing 5 µg DNA was injected into TA muscles. Injected muscles were then electroporated with electrodes placed on each side of the muscle using eight 200-V cm-1 pulses of 20 ms applied at 2 Hz (ECM 830; BTX) as previously described (Ravel-Chapuis et al., 2007).

Luciferase reporter assay

7 d after electroporation, assays for Luciferase enzymatic activity were performed on homogenized TA muscle lysates using the reporter assay system(Dual-Luciferase; Promega) according to the manufacturer's instructions. Measurements were performed using a luminometer (Lumat LB 9507; Berthold Technologies).

Nuclear–cytoplasmic fractionation

Cells were resuspended in 200 µl of fractionation buffer (0.01 M Tris-HCl, pH 7.4, 0.65% NP-40, 0.15 M NaCl, and 1.5 mM $MgCl_2$). Nuclei were pelleted, and the supernatant containing the cytoplasmic fraction was separated. The nuclear pellet was resuspended in 200 µl of fractionation buffer. Then, 50 µl of disruption buffer (0.5 M Tris-HCl, pH 8.8, 0.05 M EDTA, and 2.5% SDS) was added to the nuclear pellet and cytoplasmic fraction. Total RNA was extracted from each fraction (see previous paragraph). Purity of the nuclear and cytoplasmic fractions was assessed by qRT-PCR using U6 and Y3 primers.

Coimmunoprecipitation

24 h after transfection, whole-cell extracts were prepared from C2C12 cells in NP-40 buffer (25 mM Tris, pH 7.5, 200 mM NaCl, 0.5% NP-40,

2 mM EDTA, 2 mM $MgCl_2$, and protease inhibitors [Complete]) and precleared with protein G beads (Sigma-Aldrich). 5% of extracts were kept as the input control. Extracts were then incubated overnight at 4°C with protein G beads coated with 3 µg of specified antibodies. One sample was incubated for 20 min at 37°C with 1 µg/µl RNase A to determine whether observed interactions are RNA dependent. After four washes with NP-40 buffer, beads containing the immunoprecipitated material were collected, resuspended in 2× loading buffer, and used for Western blot analysis.

Statistical analysis

Student's *t* tests were used to determine whether differences between groups were significant. The level of significance was set at $P \leq 0.05$. In the figures, a single asterisk shows $P < 0.05$, a double asterisk shows $P < 0.01$, a triple asterisk shows $P < 0.001$, and ns represents $P > 0.05$ (Student's *t* test).

Online supplemental material

Fig. S1 shows the level of overexpression of ectopic Staufen1-HA protein compared with endogenous Staufen1. Fig. S2 shows that Staufen1 does not alter the stability of alternatively spliced IR minigene transcripts. Fig. S3 shows that Staufen1 regulates ClC-1 minigene alternative splicing. Fig. S4 shows the subcellular localization of CUG^{exp} mRNAs. Table S1 shows biopsy information used in this study. Online supplemental material is available at http://www.jcb.org/cgi/content/full/jcb.201108113/DC1.

We wish to thank our colleagues for helpful discussion throughout the course of this work. We are also indebted to Drs. T. Cooper, A. MacKenzie, R. Pelletier, M. Rudnicki, C. Thornton, and N. Webster for providing us with reagents for this study. We also thank J. Lunde for technical assistance.

This work was supported by the Canadian Institutes of Health Research (CIHR) and the Rachel Fund (CIHR–Institute of Musculoskeletal Health and Arthritis and Muscular Dystrophy Canada). J. Côté holds a Tier II Canada Research Chair in RNA Metabolism funded through CIHR. A. Ravel-Chapuis was a recipient of a Postdoctoral Fellowship from the Association Française contre les Myopathies and from the CIHR and is now supported by a Development Grant from the Muscular Dystrophy Association.

Submitted: 18 August 2011
Accepted: 17 February 2012

References

Amack, J.D., and M.S. Mahadevan. 2001. The myotonic dystrophy expanded CUG repeat tract is necessary but not sufficient to disrupt C2C12 myoblast differentiation. *Hum. Mol. Genet.* 10:1879–1887. http://dx.doi.org/10.1093/hmg/10.18.1879

Bélanger, G., M.A. Stocksley, M. Vandromme, L. Schaeffer, L. Furic, L. DesGroseillers, and B.J. Jasmin. 2003. Localization of the RNA-binding proteins Staufen1 and Staufen2 at the mammalian neuromuscular junction. *J. Neurochem.* 86:669–677. http://dx.doi.org/10.1046/j.1471-4159.2003.01883.x

Buj-Bello, A., D. Furling, H. Tronchère, J. Laporte, T. Lerouge, G.S. Butler-Browne, and J.L. Mandel. 2002. Muscle-specific alternative splicing of myotubularin-related 1 gene is impaired in DM1 muscle cells. *Hum. Mol. Genet.* 11:2297–2307. http://dx.doi.org/10.1093/hmg/11.19.2297

Charlet-B, N., R.S. Savkur, G. Singh, A.V. Philips, E.A. Grice, and T.A. Cooper. 2002. Loss of the muscle-specific chloride channel in type 1 myotonic dystrophy due to misregulated alternative splicing. *Mol. Cell.* 10:45–53. http://dx.doi.org/10.1016/S1097-2765(02)00572-5

Cooper, T.A. 2005. Use of minigene systems to dissect alternative splicing elements. *Methods.* 37:331–340. http://dx.doi.org/10.1016/j.ymeth.2005.07.015

Coté, J., S. Dupuis, Z. Jiang, and J.Y. Wu. 2001. Caspase-2 pre-mRNA alternative splicing: Identification of an intronic element containing a decoy 3′ acceptor site. *Proc. Natl. Acad. Sci. USA.* 98:938–943. http://dx.doi.org/10.1073/pnas.031564098

Dugré-Brisson, S., G. Elvira, K. Boulay, L. Chatel-Chaix, A.J. Mouland, and L. DesGroseillers. 2005. Interaction of Staufen1 with the 5′ end of mRNA facilitates translation of these RNAs. *Nucleic Acids Res.* 33:4797–4812. http://dx.doi.org/10.1093/nar/gki794

François, V., A.F. Klein, C. Beley, A. Jollet, C. Lemercier, L. Garcia, and D. Furling. 2011. Selective silencing of mutated mRNAs in DM1 by using modified hU7-snRNAs. *Nat. Struct. Mol. Biol.* 18:85–87. http://dx.doi.org/10.1038/nsmb.1958

Ho, T.H., N. Charlet-B, M.G. Poulos, G. Singh, M.S. Swanson, and T.A. Cooper. 2004. Muscleblind proteins regulate alternative splicing. *EMBO J.* 23:3103–3112. http://dx.doi.org/10.1038/sj.emboj.7600300

Ho, T.H., D. Bundman, D.L. Armstrong, and T.A. Cooper. 2005. Transgenic mice expressing CUG-BP1 reproduce splicing mis-regulation observed in myotonic dystrophy. *Hum. Mol. Genet.* 14:1539–1547. http://dx.doi.org/10.1093/hmg/ddi162

Jones, K., B. Jin, P. Iakova, C. Huichalaf, P. Sarkar, C. Schneider-Gold, B. Schoser, G. Meola, A.B. Shyu, N. Timchenko, and L. Timchenko. 2011. RNA Foci, CUGBP1, and ZNF9 are the primary targets of the mutant CUG and CCUG repeats expanded in myotonic dystrophies type 1 and type 2. *Am. J. Pathol.* 179:2475–2489. http://dx.doi.org/10.1016/j.ajpath.2011.07.013

Kanadia, R.N., K.A. Johnstone, A. Mankodi, C. Lungu, C.A. Thornton, D. Esson, A.M. Timmers, W.W. Hauswirth, and M.S. Swanson. 2003. A muscleblind knockout model for myotonic dystrophy. *Science.* 302:1978–1980. http://dx.doi.org/10.1126/science.1088583

Kiebler, M.A., I. Hemraj, P. Verkade, M. Köhrmann, P. Fortes, R.M. Marión, J. Ortín, and C.G. Dotti. 1999. The mammalian staufen protein localizes to the somatodendritic domain of cultured hippocampal neurons: implications for its involvement in mRNA transport. *J. Neurosci.* 19:288–297.

Kim, D.H., M.A. Langlois, K.B. Lee, A.D. Riggs, J. Puymirat, and J.J. Rossi. 2005a. HnRNP H inhibits nuclear export of mRNA containing expanded CUG repeats and a distal branch point sequence. *Nucleic Acids Res.* 33:3866–3874. http://dx.doi.org/10.1093/nar/gki698

Kim, Y.K., L. Furic, L. DesGroseillers, and L.E. Maquat. 2005b. Mammalian Staufen1 recruits Upf1 to specific mRNA 3'UTRs so as to elicit mRNA decay. *Cell.* 120:195–208. http://dx.doi.org/10.1016/j.cell.2004.11.050

Kim, Y.K., L. Furic, M. Parisien, F. Major, L. DesGroseillers, and L.E. Maquat. 2007. Staufen1 regulates diverse classes of mammalian transcripts. *EMBO J.* 26:2670–2681. http://dx.doi.org/10.1038/sj.emboj.7601712

Kosaki, A., J. Nelson, and N.J. Webster. 1998. Identification of intron and exon sequences involved in alternative splicing of insulin receptor pre-mRNA. *J. Biol. Chem.* 273:10331–10337. http://dx.doi.org/10.1074/jbc.273.17.10331

Kuyumcu-Martinez, N.M., G.S. Wang, and T.A. Cooper. 2007. Increased steady-state levels of CUGBP1 in myotonic dystrophy 1 are due to PKC-mediated hyperphosphorylation. *Mol. Cell.* 28:68–78. http://dx.doi.org/10.1016/j.molcel.2007.07.027

Le, S., R. Sternglanz, and C.W. Greider. 2000. Identification of two RNA-binding proteins associated with human telomerase RNA. *Mol. Biol. Cell.* 11:999–1010.

Lee, J.E., and T.A. Cooper. 2009. Pathogenic mechanisms of myotonic dystrophy. *Biochem. Soc. Trans.* 37:1281–1286. http://dx.doi.org/10.1042/BST0371281

Lin, X., J.W. Miller, A. Mankodi, R.N. Kanadia, Y. Yuan, R.T. Moxley, M.S. Swanson, and C.A. Thornton. 2006. Failure of MBNL1-dependent post-natal splicing transitions in myotonic dystrophy. *Hum. Mol. Genet.* 15:2087–2097. http://dx.doi.org/10.1093/hmg/ddl132

Luo, M., T.F. Duchaîne, and L. DesGroseillers. 2002. Molecular mapping of the determinants involved in human Staufen-ribosome association. *Biochem. J.* 365:817–824. http://dx.doi.org/10.1042/BJ20020263

Magaña, J.J., and B. Cisneros. 2011. Perspectives on gene therapy in myotonic dystrophy type 1. *J. Neurosci. Res.* 89:275–285. http://dx.doi.org/10.1002/jnr.22551

Mahadevan, M.S., R.S. Yadava, Q. Yu, S. Balijepalli, C.D. Frenzel-McCardell, T.D. Bourne, and L.H. Phillips. 2006. Reversible model of RNA toxicity and cardiac conduction defects in myotonic dystrophy. *Nat. Genet.* 38:1066–1070. http://dx.doi.org/10.1038/ng1857

Mankodi, A., E. Logigian, L. Callahan, C. McClain, R. White, D. Henderson, M. Krym, and C.A. Thornton. 2000. Myotonic dystrophy in transgenic mice expressing an expanded CUG repeat. *Science.* 289:1769–1773. http://dx.doi.org/10.1126/science.289.5485.1769

Mankodi, A., M.P. Takahashi, H. Jiang, C.L. Beck, W.J. Bowers, R.T. Moxley, S.C. Cannon, and C.A. Thornton. 2002. Expanded CUG repeats trigger aberrant splicing of ClC-1 chloride channel pre-mRNA and hyperexcitability of skeletal muscle in myotonic dystrophy. *Mol. Cell.* 10:35–44. http://dx.doi.org/10.1016/S1097-2765(02)00563-4

Marión, R.M., P. Fortes, A. Beloso, C. Dotti, and J. Ortín. 1999. A human sequence homologue of Staufen is an RNA-binding protein that is associated with polysomes and localizes to the rough endoplasmic reticulum. *Mol. Cell. Biol.* 19:2212–2219.

Martel, C., P. Macchi, L. Furic, M.A. Kiebler, and L. DesGroseillers. 2006. Staufen1 is imported into the nucleolus via a bipartite nuclear localization signal and several modulatory determinants. *Biochem. J.* 393:245–254. http://dx.doi.org/10.1042/BJ20050694

Martel, C., S. Dugré-Brisson, K. Boulay, B. Breton, G. Lapointe, S. Armando, V. Trépanier, T. Duchaîne, M. Bouvier, and L. DesGroseillers. 2010.

Multimerization of Staufen1 in live cells. *RNA*. 16:585–597. http://dx.doi.org/10.1261/rna.1664210

Michalowski, S., J.W. Miller, C.R. Urbinati, M. Paliouras, M.S. Swanson, and J. Griffith. 1999. Visualization of double-stranded RNAs from the myotonic dystrophy protein kinase gene and interactions with CUG-binding protein. *Nucleic Acids Res.* 27:3534–3542. http://dx.doi.org/10.1093/nar/27.17.3534

Miller, J.W., C.R. Urbinati, P. Teng-Umnuay, M.G. Stenberg, B.J. Byrne, C.A. Thornton, and M.S. Swanson. 2000. Recruitment of human muscleblind proteins to (CUG)(n) expansions associated with myotonic dystrophy. *EMBO J.* 19:4439–4448. http://dx.doi.org/10.1093/emboj/19.17.4439

Orengo, J.P., P. Chambon, D. Metzger, D.R. Mosier, G.J. Snipes, and T.A. Cooper. 2008. Expanded CTG repeats within the DMPK 3′ UTR causes severe skeletal muscle wasting in an inducible mouse model for myotonic dystrophy. *Proc. Natl. Acad. Sci. USA*. 105:2646–2651. http://dx.doi.org/10.1073/pnas.0708519105

O'Rourke, J.R., and M.S. Swanson. 2009. Mechanisms of RNA-mediated disease. *J. Biol. Chem.* 284:7419–7423. http://dx.doi.org/10.1074/jbc.R800025200

Paul, S., W. Dansithong, D. Kim, J. Rossi, N.J. Webster, L. Comai, and S. Reddy. 2006. Interaction of muscleblind, CUG-BP1 and hnRNP H proteins in DM1-associated aberrant IR splicing. *EMBO J.* 25:4271–4283. http://dx.doi.org/10.1038/sj.emboj.7601296

Querido, E., F. Gallardo, M. Beaudoin, C. Ménard, and P. Chartrand. 2011. Stochastic and reversible aggregation of mRNA with expanded CUG-triplet repeats. *J. Cell Sci.* 124:1703–1714. http://dx.doi.org/10.1242/jcs.073270

Ranum, L.P., and T.A. Cooper. 2006. RNA-mediated neuromuscular disorders. *Annu. Rev. Neurosci.* 29:259–277. http://dx.doi.org/10.1146/annurev.neuro.29.051605.113014

Rau, F., F. Freyermuth, C. Fugier, J.P. Villemin, M.C. Fischer, B. Jost, D. Dembele, G. Gourdon, A. Nicole, D. Duboc, et al. 2011. Misregulation of miR-1 processing is associated with heart defects in myotonic dystrophy. *Nat. Struct. Mol. Biol.* 18:840–845. http://dx.doi.org/10.1038/nsmb.2067

Ravel-Chapuis, A., M. Vandromme, J.L. Thomas, and L. Schaeffer. 2007. Postsynaptic chromatin is under neural control at the neuromuscular junction. *EMBO J.* 26:1117–1128. http://dx.doi.org/10.1038/sj.emboj.7601572

Savkur, R.S., A.V. Philips, and T.A. Cooper. 2001. Aberrant regulation of insulin receptor alternative splicing is associated with insulin resistance in myotonic dystrophy. *Nat. Genet.* 29:40–47. http://dx.doi.org/10.1038/ng704

Schoser, B., and L. Timchenko. 2010. Myotonic dystrophies 1 and 2: complex diseases with complex mechanisms. *Curr. Genomics*. 11:77–90. http://dx.doi.org/10.2174/138920210790886844

Seznec, H., O. Agbulut, N. Sergeant, C. Savouret, A. Ghestem, N. Tabti, J.C. Willer, L. Ourth, C. Duros, E. Brisson, et al. 2001. Mice transgenic for the human myotonic dystrophy region with expanded CTG repeats display muscular and brain abnormalities. *Hum. Mol. Genet.* 10:2717–2726. http://dx.doi.org/10.1093/hmg/10.23.2717

Tian, B., R.J. White, T. Xia, S. Welle, D.H. Turner, M.B. Mathews, and C.A. Thornton. 2000. Expanded CUG repeat RNAs form hairpins that activate the double-stranded RNA-dependent protein kinase PKR. *RNA*. 6:79–87. http://dx.doi.org/10.1017/S1355838200991544

Timchenko, L.T., N.A. Timchenko, C.T. Caskey, and R. Roberts. 1996. Novel proteins with binding specificity for DNA CTG repeats and RNA CUG repeats: implications for myotonic dystrophy. *Hum. Mol. Genet.* 5:115–121. http://dx.doi.org/10.1093/hmg/5.1.115

Timchenko, N.A., P. Iakova, Z.J. Cai, J.R. Smith, and L.T. Timchenko. 2001. Molecular basis for impaired muscle differentiation in myotonic dystrophy. *Mol. Cell. Biol.* 21:6927–6938. http://dx.doi.org/10.1128/MCB.21.20.6927-6938.2001

Timchenko, N.A., R. Patel, P. Iakova, Z.J. Cai, L. Quan, and L.T. Timchenko. 2004. Overexpression of CUG triplet repeat-binding protein, CUGBP1, in mice inhibits myogenesis. *J. Biol. Chem.* 279:13129–13139. http://dx.doi.org/10.1074/jbc.M312923200

Warf, M.B., and J.A. Berglund. 2007. MBNL binds similar RNA structures in the CUG repeats of myotonic dystrophy and its pre-mRNA substrate cardiac troponin T. *RNA*. 13:2238–2251. http://dx.doi.org/10.1261/rna.610607

Warf, M.B., J.V. Diegel, P.H. von Hippel, and J.A. Berglund. 2009. The protein factors MBNL1 and U2AF65 bind alternative RNA structures to regulate splicing. *Proc. Natl. Acad. Sci. USA*. 106:9203–9208. http://dx.doi.org/10.1073/pnas.0900342106

Wheeler, T.M., and C.A. Thornton. 2007. Myotonic dystrophy: RNA-mediated muscle disease. *Curr. Opin. Neurol.* 20:572–576. http://dx.doi.org/10.1097/WCO.0b013e3282ef6064

Wheeler, T.M., K. Sobczak, J.D. Lueck, R.J. Osborne, X. Lin, R.T. Dirksen, and C.A. Thornton. 2009. Reversal of RNA dominance by displacement of protein sequestered on triplet repeat RNA. *Science*. 325:336–339. http://dx.doi.org/10.1126/science.1173110

Wickham, L., T. Duchaîne, M. Luo, I.R. Nabi, and L. DesGroseillers. 1999. Mammalian staufen is a double-stranded-RNA- and tubulin-binding protein which localizes to the rough endoplasmic reticulum. *Mol. Cell. Biol.* 19:2220–2230.

Yuan, Y., S.A. Compton, K. Sobczak, M.G. Stenberg, C.A. Thornton, J.D. Griffith, and M.S. Swanson. 2007. Muscleblind-like 1 interacts with RNA hairpins in splicing target and pathogenic RNAs. *Nucleic Acids Res.* 35:5474–5486. http://dx.doi.org/10.1093/nar/gkm601